Raloxifene and Bazedoxifene as Selective ALDH1A1 Inhibitors to Ameliorate Cyclophosphamide Resistance: A Drug Repurposing Approach

1. Introduction

Cyclophosphamide (CP), is a popular therapeutic option for a variety of malignancies, including chronic lymphocytic leukemia, chronic myelocytic leukemia, acute myeloid leukemia, breast cancer, and ovarian cancer [1]. However, cancer chemotherapy is often weighed down by drug resistance that hinders effective treatment [2]. Several reports indicated CP suffers from the problem of resistance via efflux, ineffective uptake, and inactivation via tumoral drug-metabolizing enzymes (DME) [3-5]. Currently, CP resistance via the inactivation mechanism is of great interest among researchers. As per the literature, DME aldehyde dehydrogenases (ALDHs) are primarily involved in CP inactivation [6].

ALDHs are phase-I oxidase enzymes that catalyze the $NAD(P)^+$-dependent oxidation of aldehydes (R-C(=O)-H) to acids (R-C(=O)-OH) [7]. These are involved in detoxifying various endogenous and exogenous compounds such as retinaldehyde, acetaldehyde, neurotransmitters, carbohydrates, and lipids [8]. The erratic biological activity of ALDHs and their role in metabolic pathways have been linked to a range of diseases, including alcoholic liver diseases and cancer [9-11]. Several studies have manifested that overexpression of certain ALDHs, especially ALDH1A1, in a variety of tumors is associated with CP resistance [12, 13]. CP is a prodrug that gets converted into 4-hydroxycyclophosphamide (4-OH CP) by a group of hepatic CYP_{450} and subsequently, bio transforms to its tautomer aldophosphamide, an active intermediate. This intermediate permeates into the cell and is converted into the active metabolite, i.e., phosphoramide mustard (PM), through spontaneous β-elimination [14]. However, the conversion of CP to PM is shunted at the aldophosphamide stage due to its conversion into an inert metabolite carboxyphosphamide via ALDH1A1 [15]. Several shreds of evidence suggest that ALDH1A1 overexpression is dependent on genetic variations, protein-protein interactions, and transcription factors [16, 17]. These factors, associated with ALDH1A1 overexpression, eventually trigger CP inactivation. The detailed mechanism of ALDH1A1 overexpression and its mediated CP inactivation is displayed in **Fig. 1**. In many studies, it has been reported that ALDH1A1 knockdown ameliorates CP sensitivity by reducing ALDH1A1-mediated metabolism. For instance, Muramoto et al reported that inhibition

of ALDH1A1 activity in murine pluripotent hematopoietic stem cells and myeloid progenitor cells correlated well with increased *in-vitro* sensitivity to 4-OH CP [18].

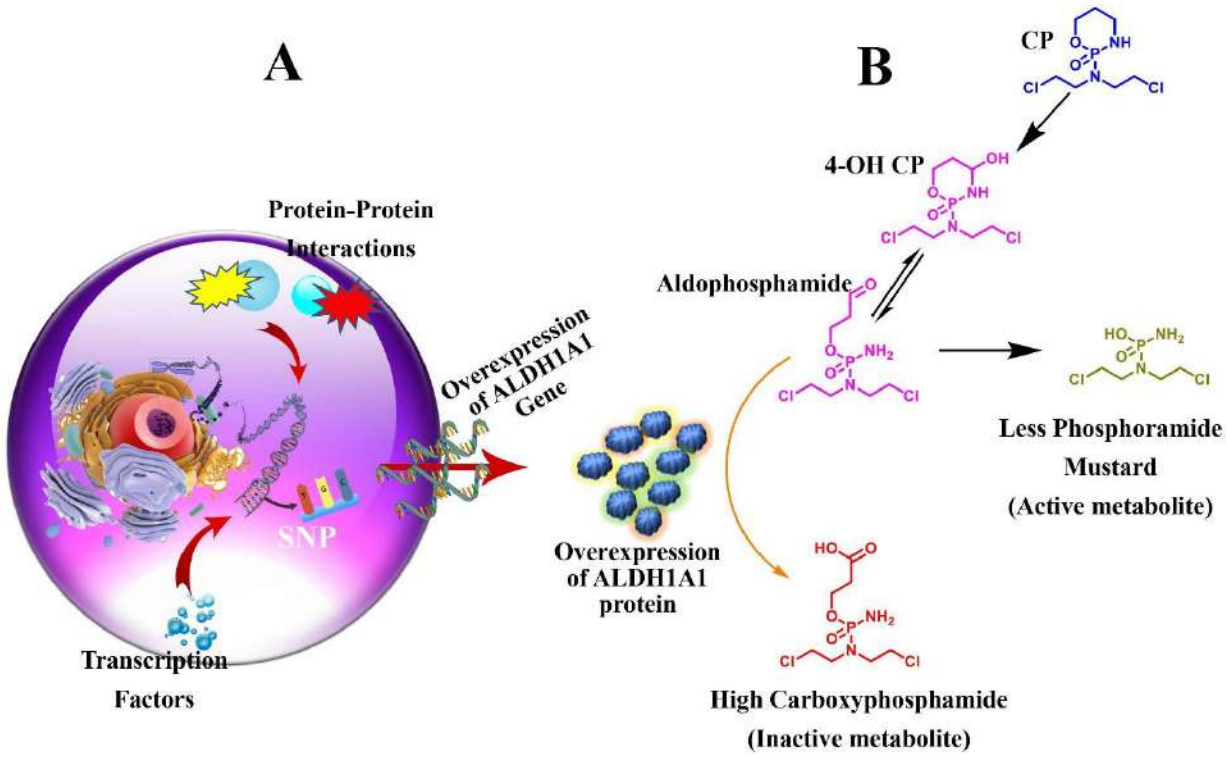

Figure 1: Factors regulating ALDH1A1 overexpression and its mediated CP inactivation via **A)** protein-protein interactions, transcription factors, and SNPs, **B)** Conversion of CP into 4-OH CP and subsequently to its tautomer aldophosphamide, which undergoes inactivation to carboxyphosphamide via ALDH1A1 leaving scanty of active metabolite i. e. phosphoramide mustard for anti-cancer activity.

Understanding the utility of exploring ALDH1A1 as a target, various research groups have reported ALDH1A1 inhibitors belonging to diverse chemical classes including theophyllines, indole-2,3-diones, aromatic lactones, pyrimidones, quinolines, and 3H-xanthen-3-ones [19-24]. Among them, NCT-501, a theophylline-based compound, is reported as a selective ALDH1A1 inhibitor with excellent inhibitory activity. However, the pharmacokinetic investigations revealed that NCT-501 possesses a short half-life of <1 hour. Such results highlight the difficulty in the development of novel ALDH1A1 inhibitors [25]. Hence, to obtain selective ALDH1A1 inhibitors

with well-established pharmacokinetic, safety, and toxicity profiles, herein drug repurposing approach has been explored [26, 27]. The FDA-approved drugs in the ZINC database were virtually screened via machine learning (ML) models reported by our research group [28] to identify promising ALDH1A1 inhibitors. The obtained hits were further subjected to structure-based drug-designing approaches, including molecular docking, molecular dynamics (MD), and WaterSwap analysis. Finally, *in-vitro* enzymatic and cell line studies were carried out for the identified drugs to validate the computational results and suggest appropriate solutions to CP resistance.

2. Objectives

1. Data mining for small and macromolecules from the database for *in-silico* evaluation
2. To perform virtual screening for ALDH1A1 inhibitors using previously validated machine learning models
3. To design small molecule inhibitors for ALDH1A1 using structure-based *in-silico* analyses and subsequent biological evaluation

3. Material and Methods

3.1. FDA-approved drug collection and preparation

A total of 1600 FDA-approved drugs were retrieved from the ZINC database [29]. The structure files for the molecules were downloaded in SDF format. The collected 2D structures were converted into 3D structures using the Spark module of Cresset software. The obtained 3D molecules were further subjected to ligand preparation to add explicit hydrogens. Once the ligand preparation was performed, PaDEL software was used to generate the 1D, 2D, and 3D descriptors for prepared 3D structures of FDA-approved drugs [30]. The generated descriptor file was later used for ML-based virtual screening (VS).

3.2. Virtual Screening

Previously developed and reported multiple ML models (ALDH1A1, ALDH2, and ALDH3A1) were utilized to screen FDA-approved drugs [28]. The screening process was conducted using the same protocol as discussed in our previous work [28]. Briefly, the ALDH1A1 model was utilized to screen a total of 1600 FDA-approved drugs as putative ALDH1A1 inhibitors. Later, the

identified ALDH1A1 inhibitors were screened through validated ALDH2 and ALDH3A1 models to eliminate non-selective inhibitors. Finally, to establish their mechanism of binding with ALDH1A1 and ensure the retention of crucial interactions, molecular docking was carried out.

3.3.Molecular Docking

3D crystal structure of ALDH1A1 i.e. 4X4L was retrieved from the RCSB Protein Data Bank (PDB) [31]. Our research group has selected 4X4L based on cross-docking experimentation. The cross-docking protocol has been briefly explained in our recently published paper [28]. This experimentation included five 3D crystal structures of ALDH1A1 with resolution <2 Å. All the selected crystal structures were aligned and subsequently, ligands from each crystal structure were extracted and redocked in the active site of each crystal structure. The root mean square deviation (RMSD) between the redocked crystal ligands and their native crystal conformations was computed. Based on the cross-docking analysis, the protein structure with a low average RMSD of redocked ligands i.e. 4X4L was considered for docking studies [28]. The crystal structure selected from redocking studies was prepared using the Flare module by following the insertion of missing atoms in incomplete residues, modeling the missing loops, removal of co-crystallized water, and protonation of the residues by applying a LeadFinder's force field [32]. The binding site is defined around the centroid of the co-crystallized ligand for the generation of the grid. Finally, docking was performed in the active site of the protein using BioMolTech's Lead Finder docking algorithm.

3.4. Molecular Dynamics

The binding modes obtained from the molecular docking analysis only provide the least energy-stable conformation of a ligand within the receptor along with key electrostatic and hydrophobic interactions. To further ensure the ligand stability within the active site of ALDH1A1, MD study was carried out using the Flare module in Cresset Software [32]. For this, the biomolecular complex was solvated in an orthorhombic box with 10 Å dimensions using the TIP3P water molecules system. The AMBER force field in Flare was applied to the protein-ligand system. Once the system was minimized, MD simulations for the period of 100 ns were carried out under the NPT ensemble with a temperature setting of 300° K and recording intervals of 2 ps throughout the simulation period. After the completion of MD, the binding orientations of the ligands within the active site of the protein and RMSD trajectories were further analyzed.

3.5. Energy Calculations

The binding affinity of ALDH1A1 towards obtained top hits was determined using WaterSwap analysis available in the Flare module of Cresset software [33, 34]. WaterSwap is a technique based on Monte Carlo (MC) simulation that is generally employed to investigate ligand-protein interactions and further calculate the absolute protein-ligand binding free energies. WaterSwap in Flare employs condensed-phase simulations using the AMBER force field. The starting conformation for WaterSwap was chosen from the final conformation obtained after MD simulations. It works by swapping the ligand bound to the protein with an equivalent shape and volume of bulk water. The binding free energy is then calculated by three different methods, such as Bennett, thermodynamics integration (TI), and free energy perturbation (FEF). A consensus of binding free energy obtained by the arithmetic mean of Bennett, TI, and FEP has been considered as total binding energy.

3.6. ALDH isoform-specific enzymatic assay

Human ALDH1A1, ALDH2, and ALDH3A1 enzymes were purchased from Abcam. The FDA-approved drugs avanafil and betrixaban were purchased from Sigma Aldrich. While raloxifene and bazadoxifene were purchased from Vivan Life Sci. Pvt. Ltd., Mumbai. The standard inhibitors NCT-501 and CB29 were purchased from Sigma Aldrich. The ALDH2 inhibitor disulfiram was received as a gift sample from Tripada Healthcare Pvt. Ltd., Ahmedabad, India. The other required chemicals including Beta-nicotinamide adenine dinucleotide and DTT were purchased from Sigma Aldrich.

The inhibitory activity of ALDH isoforms was assayed spectrophotometrically by monitoring the formation of NADH at 340 nm. Briefly, 1 μg/mL ALDH1A1 was dispatched into a 96-well plate. Later, the enzyme plate was treated with different concentrations of FDA-approved drugs, standard inhibitors, and control were incubated for 15 minutes at 25°C. The reaction was initiated by the addition of a substrate mixture containing 10 mM propionaldehyde, 2 mM DTT, 100 mM KCl, 1 mM NAD^+, and 50 mM Tris pH 8.5. Then, the absorbance of NADH was recorded in kinetic mode for 5 minutes. NCT-501 was used as a standard in the ALDH1A1 inhibition assay. Similarly, for ALDH2, 0.5 μg/mL of the enzyme was used in the reaction with 2 mM acetaldehyde as the substrate, and 0.2 μg/mL of the enzyme was used in the ALDH3A1 inhibition assay with 1 mM 4-

nitrobenzaldehyde as the substrate. Disulfiram and CB29 were used as standards in ALDH2 and ALDH3A1 reactions, respectively [22].

3.7. Mafosfamide sensitivity assay

An MTT assay was performed to identify the cytotoxicity potential of Mafosfamide (maf) alone and in the combination of test compounds among the reported ALDH1A1 overexpressing cell lines i.e. A549 and MIA PaCa [35] (Yasgar et al.,2017). Here the maf was purchased from Niomech-IIT GmbH, Germany, D-17272. Maf was chosen for this study because it is a cyclophosphamide analog that does not require cytochrome P450 to activate, making it perfect for cell-based research. Two cell lines, A549 and MIA-Paca-2, were chosen because they express high levels of ALDH1A1 [35]. A549 and MIA PaCa-2 cells were purchased from the National Centre for Cell Science (NCCS), Pune, India. The MTT assay was performed according to protocols adopted in a report published by Parajuli in 2014 [36] in BSL-3, Department of Botany and Environmental Sciences, Guru Nanak Dev University, Amritsar, India.

4. Results

4.1.Virtual Screening

4.1.1. ML and molecular docking-based VS

To identify selective ALDH1A1 inhibitors which could work as adjuvant drugs with CP, already reported ML models for ALDH1A1, ALDH2, and ALDH3A1 were utilized to screen a total of 1600 FDA-approved drugs. As a result of an initial screening from the ALDH1A1 model, around 528 molecules filtered out as ALDH1A1 inhibitors. To remove non-selective ALDH1A1 inhibitors, the obtained 528 molecules were screened from ML models for ALDH2 and ALDH3A1. Overall, a total of 115 molecules were found as selective ALDH1A1 inhibitors. The detailed combined VS protocol is displayed in **Fig. 2**. In the next step, the obtained hits were subjected to molecular docking in the active site of ALDH1A1 (PDB ID: 4X4L). The docking protocol was first validated via redocking of the co-crystallized ligand in the 4X4L structure. The poses of both redocked and co-crystallized ligands were compared and superimposed. The RMSD value of 0.49 Å was observed amongst the poses. It is reported that a maximum of ≤2.0 RMSD between the co-crystal ligand and redocked structure is considered realistic (**Fig. 3**). The same grid generated around the co-crystallized ligand was utilized for carrying out the docking of the

obtained 115 hits. Among them, a total of 13 molecules were selected based on their best Lead Finder scores (LF rank score, LF dG score, and LF VSscore) compared to what was obtained with the co-crystalized ligand of ALDH1A1 i.e., -10.16, -10.05, and -09.21, respectively. Herein, the LF rank score indicates the best ligand pose, which is similar to the experimental observation. The more negative the LF rank score is, the higher the chance that the docked poses would reproduce the crystallographic pose. The LF dG scoring function estimates the protein-ligand binding free energy in the gas phase. The LF VS score represents efficacy in the VS experiment; the more negative the score is, the higher the probability of ligands being more active. The detailed LF scores for the screened hits are enlisted in **Table 1** along with their ZINC codes. The top-scored four molecules (**Fig. 4**) were further docked against other ALDH isoforms, such as ALDH2 and ALDH3A1, to distinguish selectivity among the three isoforms and to obtain the best selective ALDH1A1 molecules. None of the molecules show better LF scores for ALDH2 and ALDH3A1 than ALDH1A1 LF scores (**Table 2** and **3**). The top four drugs, including raloxifene, bazedoxifene, avanafil, and betrixaban, could not be docked in the cavity of ALDH2 and ALDH3A1 due to their narrow and constricted cavity. This distinguished front and side surface view for the cavities of ALDH2 and ALDH3A1 can be visualized in **Fig. 5** and **6**. The top hits in the complex with ALDH1A1 were further subjected to MD simulations.

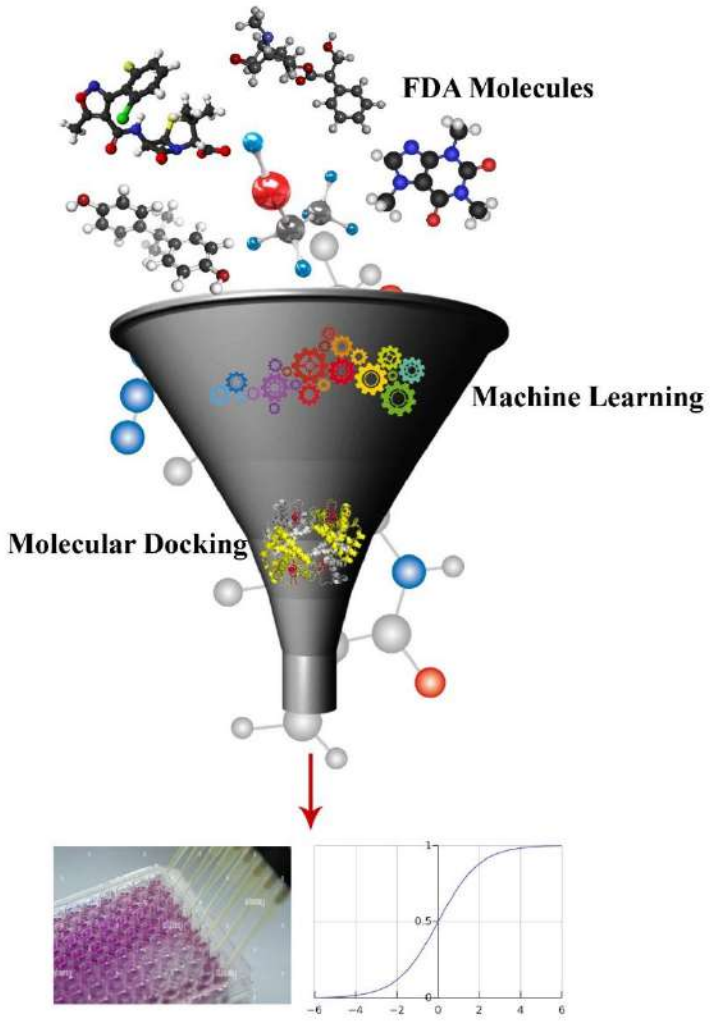

Figure 2: Brief representation of the ML- and docking-based VS protocol

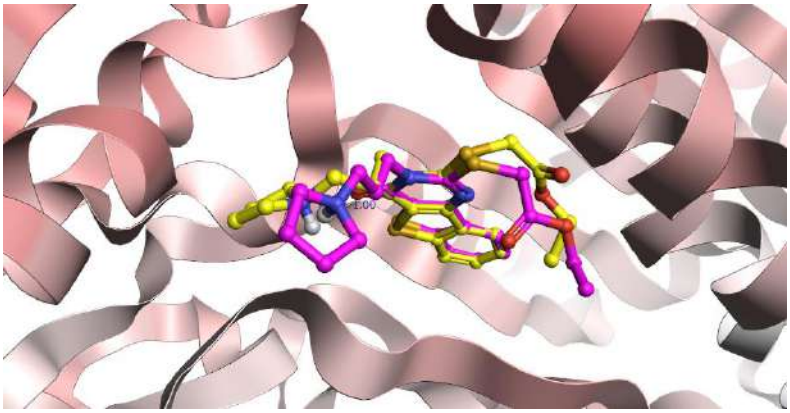

Figure 3: Comparison between ALDH1A1 cocrystal ligand (pink) and its redocked ligand pose (yellow)

Table 1: Molecular docking scores of FDA approved molecules identified towards ALDH1A1

Rank	ZINC ID	Compound Name	LF rank score[@]	LF dG score[#]	LF VSscore[$]
1	ZINC000000538275	Raloxifene	-15.55	-15.62	-16.23
2	ZINC000001895505	Bazedoxifene	-15.36	-15.44	-16.10
3	ZINC000011677857	Avanafil (Stendra)	-14.92	-15.12	-15.55
4	ZINC000030691754	Betrixaban	-13.81	-14.92	-15.24
5	ZINC000003986735	Sprycel	-12.26	-13.55	-13.28
6	ZINC000003820029	Trajenta	-11.76	-11.98	-10.36
7	ZINC000011679756	Eltrombopaq	-11.65	-11.48	-10.22
8	ZINC000011616925	Folotyn	-11.12	-10.95	-10.05
9	ZINC000084758479	Brexpiprazole	-10.84	-10-72	-10.02
10	ZINC000011617039	Pazopanib	-10.65	-10.63	-10.02
11	ZINC000008577218	Pga	-10.58	-10.42	-09.88
12	ZINC000000538658	Samsca	-10.42	-10.33	-09.72
13	ZINC000034608502	Umeclidinium	-10.21	-10.09	-09.46
14	Cocrystalized ligand	4X4L	-10.16	-10.05	-09.21

[@]Score used to rank the poses of docked compounds
[#]Score used to rank the binding energy of docked compounds in terms of kcal/mol
[$]Score used to rank the docked compounds in virtual screening

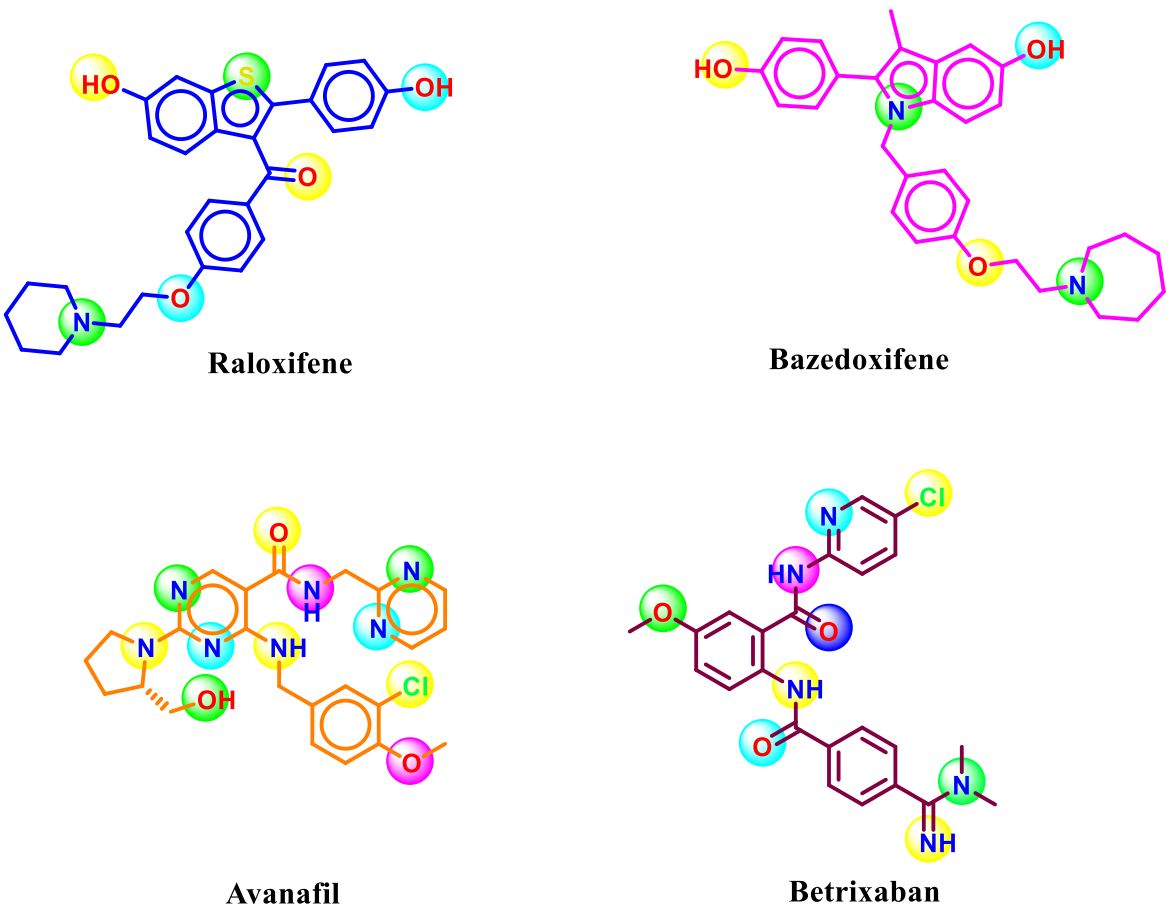

Figure 4: The best-identified top four FDA molecules as ALDH1A1 inhibitors from Virtual Screening

Table 2: Molecular docking scores of FDA-approved molecules identified towards ALDH2

Rank	ZINC ID	Compound Name	LF rank score[@]	LF dG score[#]	LF VSscore[$]
1	ZINC000000538275	Raloxifene	-1.20	-2.10	-3.83
2	ZINC000001895505	Bazedoxifene	-2.46	-3.14	-1.10
3	ZINC000011677857	Avanafil (Stendra)	1-.22	-1.12	-2.75

4	ZINC000030691754	Betrixaban	-2.01	-3.85	-1.24
5	ZINC000003986735	Sprycel	-0.26	-1.65	-1.26
6	ZINC000003820029	Trajenta	-1.73	-1.92	-0.36
7	ZINC000011679756	Eltrombopaq	-1.35	-1.58	-0.02
8	ZINC000011616925	Folotyn	-1.02	-0.95	-1.02
9	ZINC000084758479	Brexpiprazole	-0.54	-0.22	-1.05
10	ZINC000011617039	Pazopanib	-1.65	-2.83	-2.42
11	ZINC000008577218	Pga	-0.88	-0.82	-1.58
12	ZINC000000538658	Samsca	-1.49	-1.83	-0.92
13	ZINC000034608502	Umeclidinium	-1.20	-0.06	-0.43
14	Cocrystalized ligand	4X4L	-1.86	-0.05	-1.01

[@]Score used to rank the poses of docked compounds
[#]Score used to rank the binding energy of docked compounds in terms of kcal/mol
[$]Score used to rank the docked compounds in virtual screening

Table 3: Molecular docking scores ofFDA-approvedd molecules identified towards ALDH3A1

Rank	**ZINC ID**	**Compound Name**	**LF rank score[@]**	**LF dG score[#]**	**LF VSscore[$]**
1	ZINC000000538275	Raloxifene	-2.56	-0.86	-1.68
2	ZINC000001895505	Bazedoxifene	-1.86	-1.36	-3.15

3	ZINC000011677857	Avanafil (Stendra)	2-.85	-3.23	-1.56
4	ZINC000030691754	Betrixaban	-2.65	-1.36	-0.74
5	ZINC000003986735	Sprycel	-2.41	-0.22	-3.96
6	ZINC000003820029	Trajenta	-2.32	-1.66	-1.85
7	ZINC000011679756	Eltrombopaq	-2.69	-0.41	-1.69
8	ZINC000011616925	Folotyn	-2.35	-1.86	-0.21
9	ZINC000084758479	Brexpiprazole	-2.35	-1.11	-0.65
10	ZINC000011617039	Pazopanib	-2.89	-0.52	-0.89
11	ZINC000008577218	Pga	-1.86	-0.15	-1.69
12	ZINC000000538658	Samsca	-2.35	-3.25	-2.75
13	ZINC000034608502	Umeclidinium	-0.56	-0.15	-0.02
14	Cocrystalized ligand	4X4L	-0.25	-0.89	-0.56

[@]Score used to rank the poses of docked compounds
[#]Score used to rank the binding energy of docked compounds in terms of kcal/mol
[$]Score used to rank the docked compounds in virtual screening

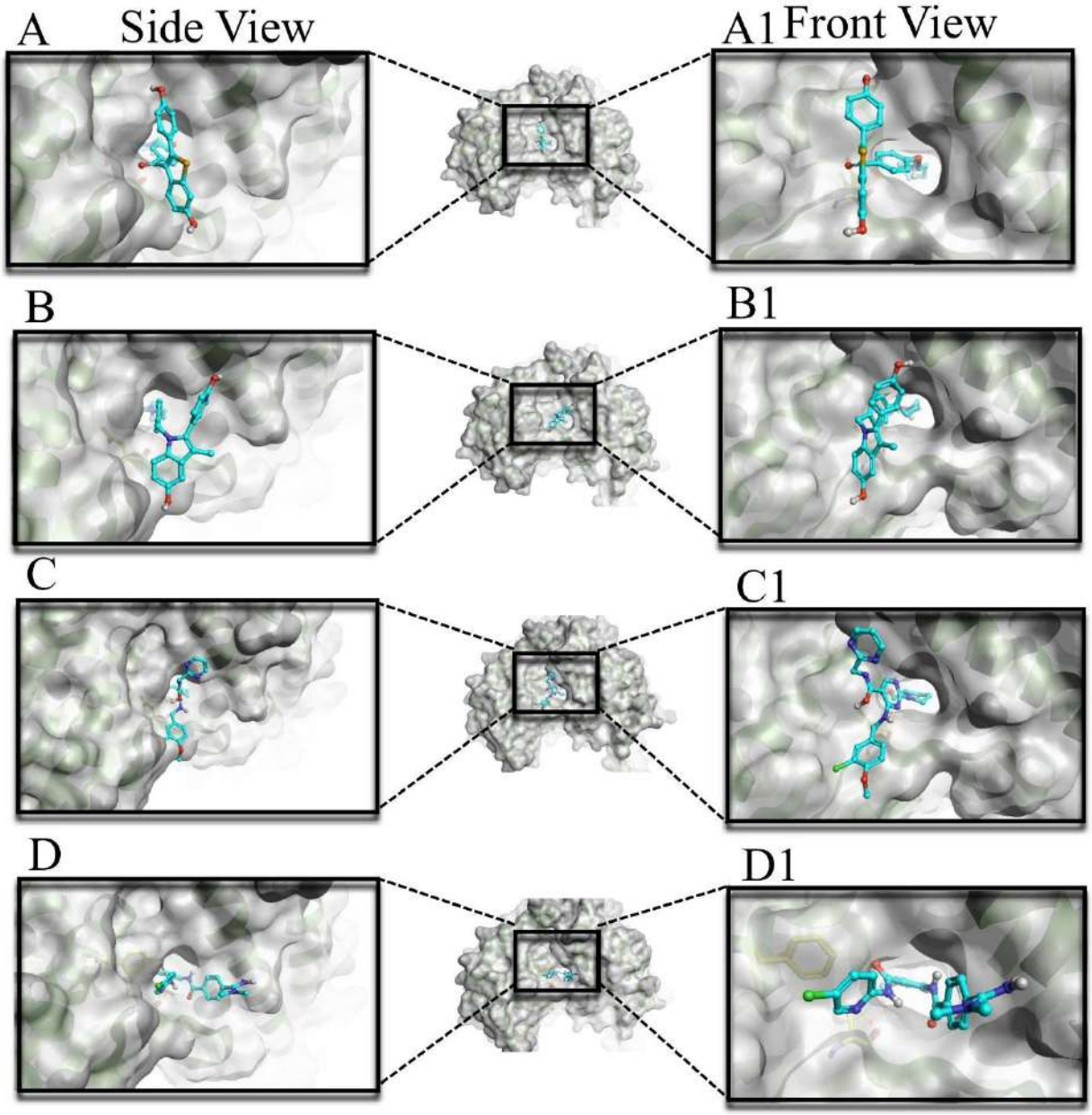

Figure 5: The binding poses of the selected FDA molecules, **A** and **A1**) raloxifene, **B** and **B1**) bazedoxifene, **C** and **C1**) avanafil, **D** and **D1**) betrixaban in the active site of ALDH2

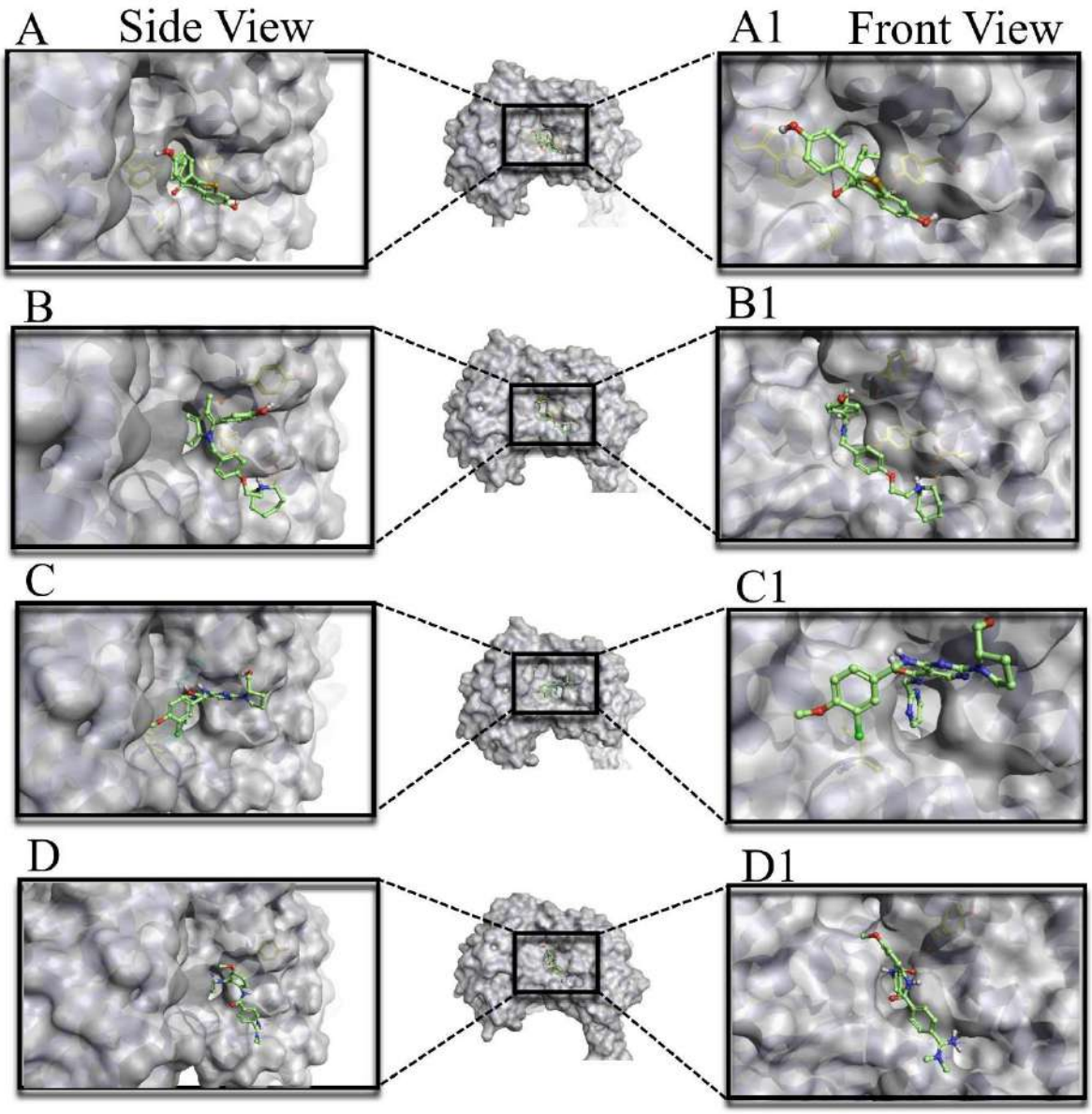

Figure 6: The binding poses of the selected FDA molecules, **A** and **A1**) raloxifene, **B** and **B1**) bazedoxifene, **C** and **C1**) avanafil, **D** and **D1**) betrixaban in the active site of ALDH3A1.

4.2. Molecular Dynamics

The MD simulation for top-docked complexes was carried out for a 100 ns period. This study further demonstrated detailed computational insights in terms of protein-ligand stability, molecular interactions, and binding modes with the target protein. The RMSD plots displayed in **Fig. 7** show that all top four complexes showed good stability throughout the simulation. During the entire

simulation, all top four complexes depicted RMSD within an allowable range i.e., <1 Å, indicating all the drugs retain the stability in complex with ALDH1A1.

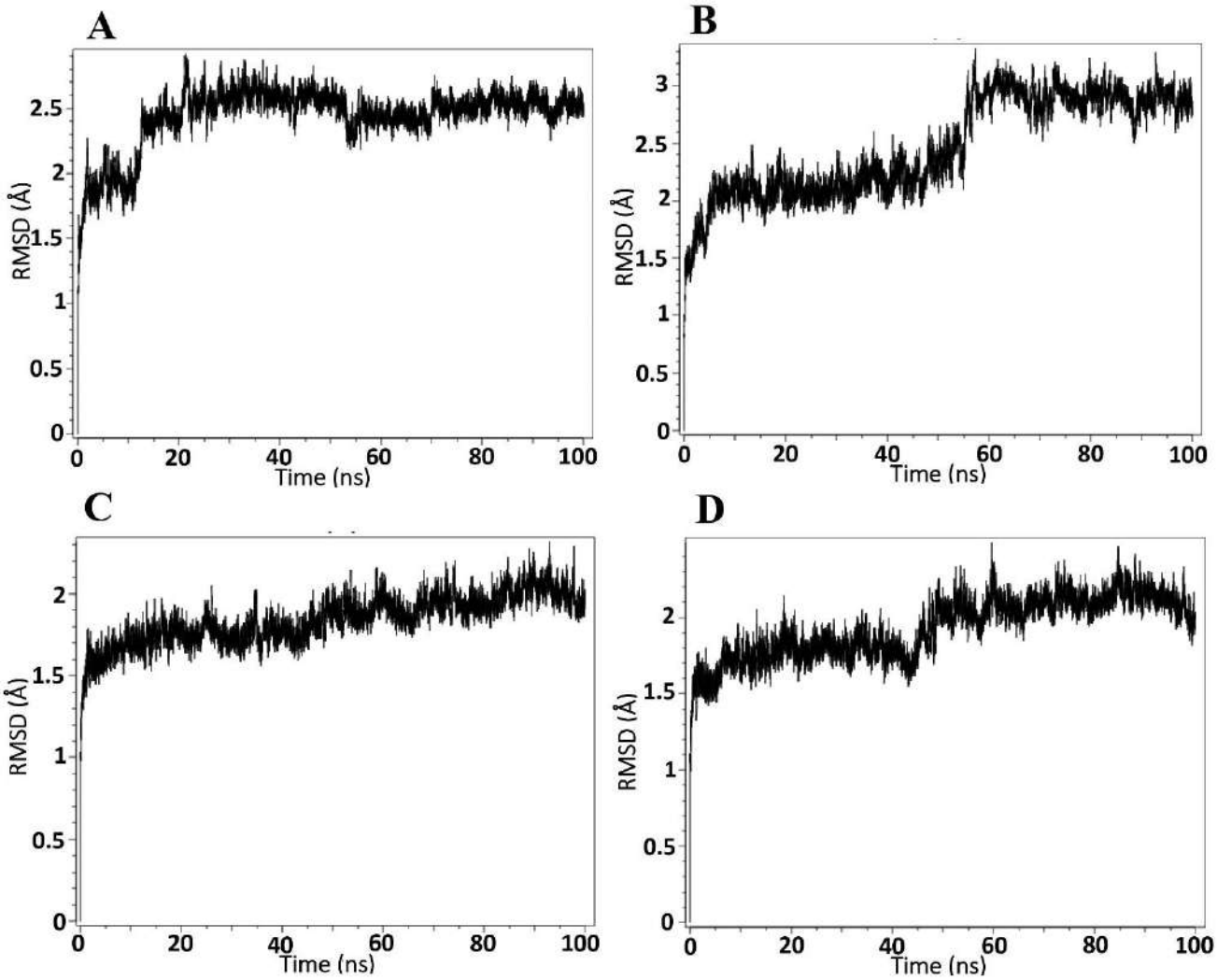

Figure 7: RMSD analysis of ALDH1A1 in complex with **A)** raloxifene **B)** bazedoxifene **C)** avanafil **D)** betrixaban

4.2.1. Interaction analysis of molecules with ALDH1A1

4.2.1.1. Raloxifene and Bazedoxifene:

The docking analysis suggested that raloxifene and bazedoxifene displayed similar interaction patterns within the active site of ALDH1A1. As observed in **Fig. 8A-8B**, the phenol moiety presents in raloxifene and bazedoxifene demonstrated pi-pi stacking interactions with Phe171. The other phenolic moieties in raloxifene and bazedoxifene have shown pi-pi interaction with Tyr297. In addition, the piperidine moiety in raloxifene displayed pi-cation interactions with Tyr297. All the docking interactions were found to be retained throughout the simulation except the interaction

between Phe171 and the phenol moiety of raloxifene. However, Phe171 came into contact with the other phenol ring of raloxifene via pi-pi interaction during the simulation and was found to be more prominent until the end of the simulation. Similarly, the pi-pi interaction between the phenol moiety on bazedoxifene and Tyr297 was maintained throughout the simulation. The pi-pi interactions with these key amino acids have already been reported to be crucial for ALDH1A1 inhibition [37, 38]. The detailed pre-and post-simulation interactions of raloxifene and bazedoxifene are displayed in **Fig. 8A** and **Fig. 9A,** and **Fig. 8B** and **Fig. 9B,** respectively**.** Moreover, the initial docking studies for raloxifene revealed two weak H-bond interactions between the hydroxy group on benzothiophene and Thr129 and Ala462, respectively. A similar kind of observation was recorded between the hydroxy group on the indole moiety of bazedoxifene and Thr129. The hydroxy group on the phenol ring in both raloxifene and bazedoxifene also demonstrated a strong H-bond interaction with Cys303. However, all the H-bond interactions disappeared after 30% of the simulation period, and observed new strong H-bond interactions between Glu255 and the hydroxy group present on the phenol ring of both raloxifene and bazedoxifene. The newly formed H-bond was considered more prominent with a % frame score value of 65%. The benzothiophene group of raloxifene and indole group of bazedoxifene show new pi-pi interactions with the important amino acid Trp178 after MD simulation. In addition, raloxifene showed a water-mediated interaction between the hydroxy group of benzothiophene and the amine group on the side chain of Trp178 at end of the simulation.

4.2.1.2. Avanafil

The pyrimidine moiety attached to pyrrolidine mainly interacted with Tyr297 via pi-pi interactions. Similarly, the phenol moiety manifested a pi-pi interaction with Phe466 during the initial period of MD simulation. The pi-pi interaction with Phe466 was maintained throughout the simulation while the pi-pi interaction between pyrrolidine and Tyr297 was maintained for ~40% of the total simulation period. Eventually, the pyrrolidine group came into contact with Phe466 and retained it until the end of the simulation. Two H-bonding interactions with Gly294 and Ser121 with a 50% frame were lost at the end of the simulation. The 3D interaction poses for avanafil before and after the simulations are illustrated in **Fig. 8C** and **Fig. 9C.**

4.2.1.3. Betrixaban

Based on the final poses obtained from pre-and post-simulation (**Fig. 8D** and **Fig. 9D**), the betrixaban interaction profiles in the ALDH1A1 active site were analyzed. During an initial period

of dynamics, the benzamide moiety in betrixaban interacted with Tyr297 which was maintained for ~20% of the simulation period, while the same in the rest of the time (80%) displayed a new interaction with His293. The benzoyl and dimethylamino groups in this drug interact with Phe466 via pi-pi interactions, and pi-cationic interactions, respectively. The same benzoyl group displays an additional pi-cationic interaction with Trp178. The % frame contact for 100 ns trajectory suggested that the observed cationic interactions retained with 43% while the pi-pi interaction between Phe466 and the benzoyl moiety manifested this score as 39%. Subsequently, a new pi-pi interaction was observed between pyridine and Phe466, which was maintained throughout the simulation.

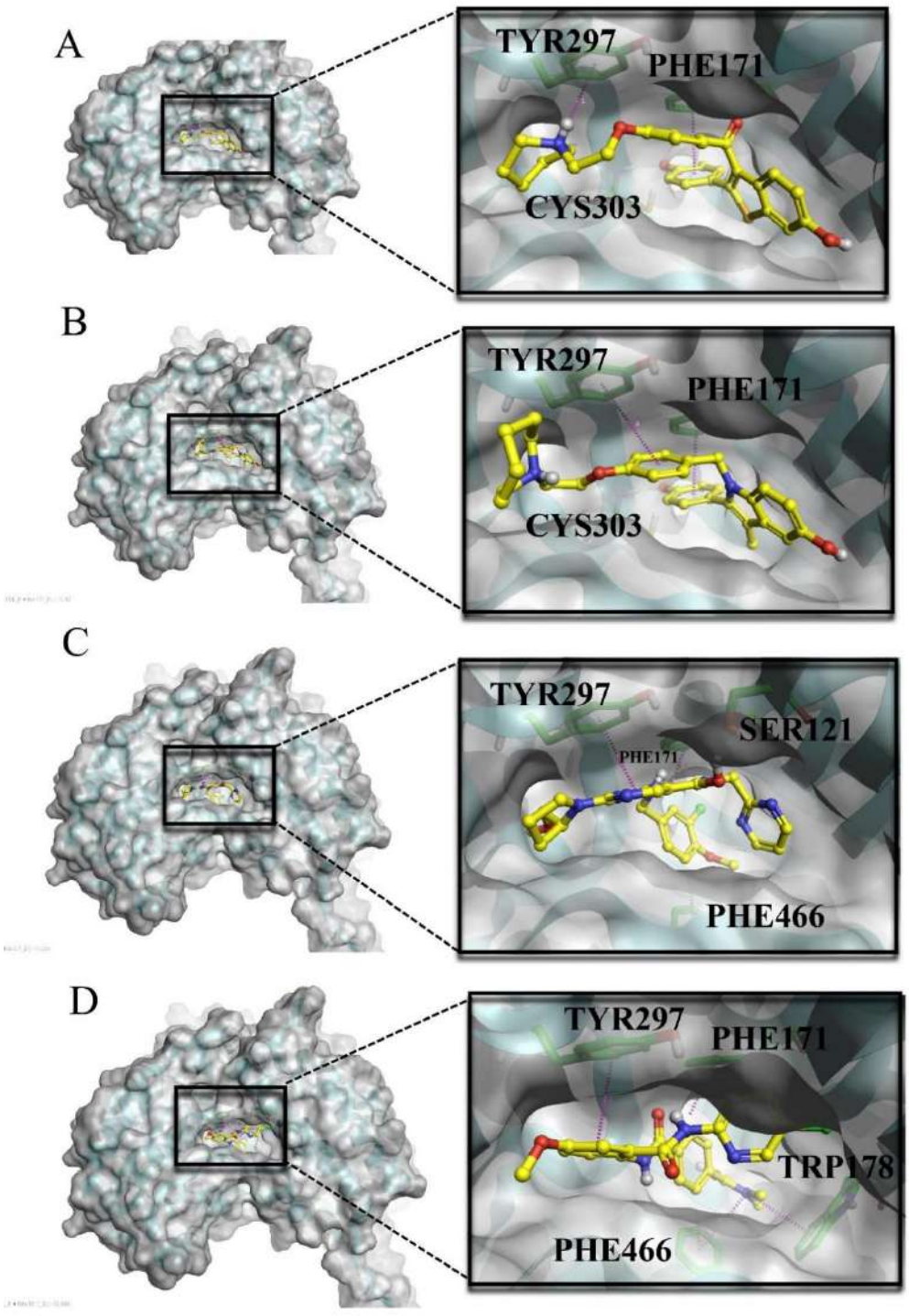

Figure 8: The binding poses of the selected FDA molecules **A**) raloxifene, **B**) bazedoxifene, **C**) avanafil, **D**) betrixaban obtained from ALDH1A1 docking, where violet represents pi-pi and pi-cation interactions, blue represents weak H-bond interactions, and the green represents strong H-bond interactions.

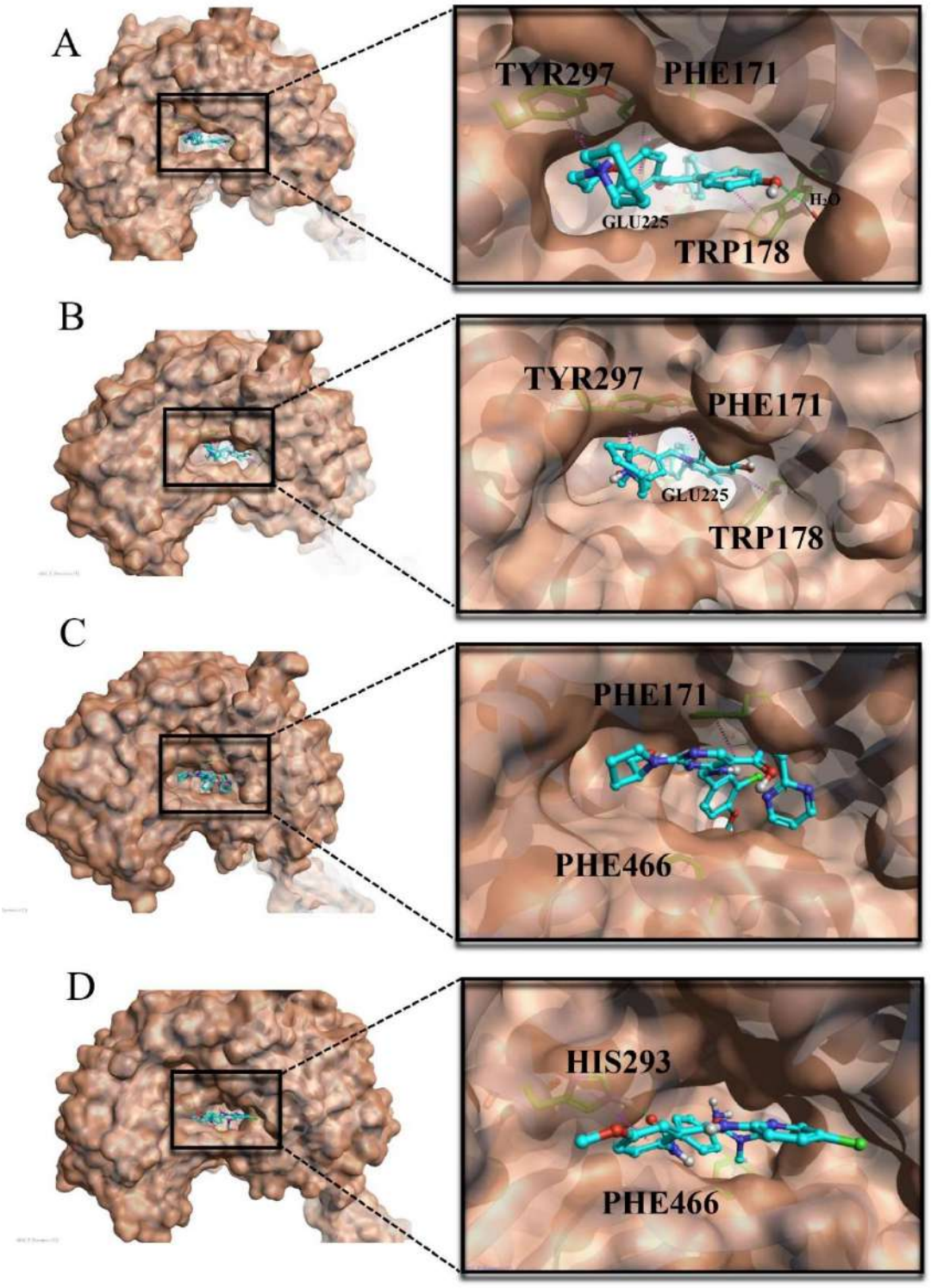

Figure 9: The binding poses of the selected FDA molecules after MD simulation **A**) raloxifene, **B**) bazedoxifene, **C**) avanafil, **D**) betrixaban in the active site of ALDH1A1

4.3. WaterSwap Analysis

WaterSwap analysis was performed to determine the binding free energy and compute the energies (ΔG, kcal/mol) for each amino acid within the active site concerning the ligand that favors the inhibition. As shown in **Fig. 10**, the green-colored amino acids are favorable for ligand interactions, and red-colored amino acids favor only the water-mediated interactions. The analysis revealed that the amino acid and ligand interactions retained after MD simulation, i.e., Tyr297, Phe171, and Glu269, were found to favorably contribute to the binding free energy for both raloxifene and bazedoxifene. The amino acid Trp178 contributed more to the water-mediated interaction for raloxifene than to the direct ligand interaction. In addition, Val460, His293, and Ser121 have been identified as additional possible hotspot amino acids for raloxifene interaction, whereas Ala462 and Gly458 have been identified as additional amino acids for bazedoxifene interaction. Furthermore, Tyr297 and Phe171 are favorable for avanafil, whereas Phe171, Ala462, and Glu255 have been identified as favorable for the betrixaban interaction with ALDH1A1. The obtained consensus of the arithmetic mean of binding energy values is -42.00 kcal/mol, -38.03 kcal/mol, -13.82 kcal/mol, and -11.48 kcal/mol for raloxifene, bazedoxifene, avanafil, and betrixaban, respectively. The detailed energy values calculated by various methods in WaterSwap analysis are illustrated in **Table 4**. The obtained results show that all the ligand complexes exhibit good binding energy. This signifies that the approved drugs might show good inhibitory potentials against ALDH1A1 in *in-vitro* experiments. To validate the *in-silico* results of drug repurposing, *in-vitro* enzymatic investigations were carried out.

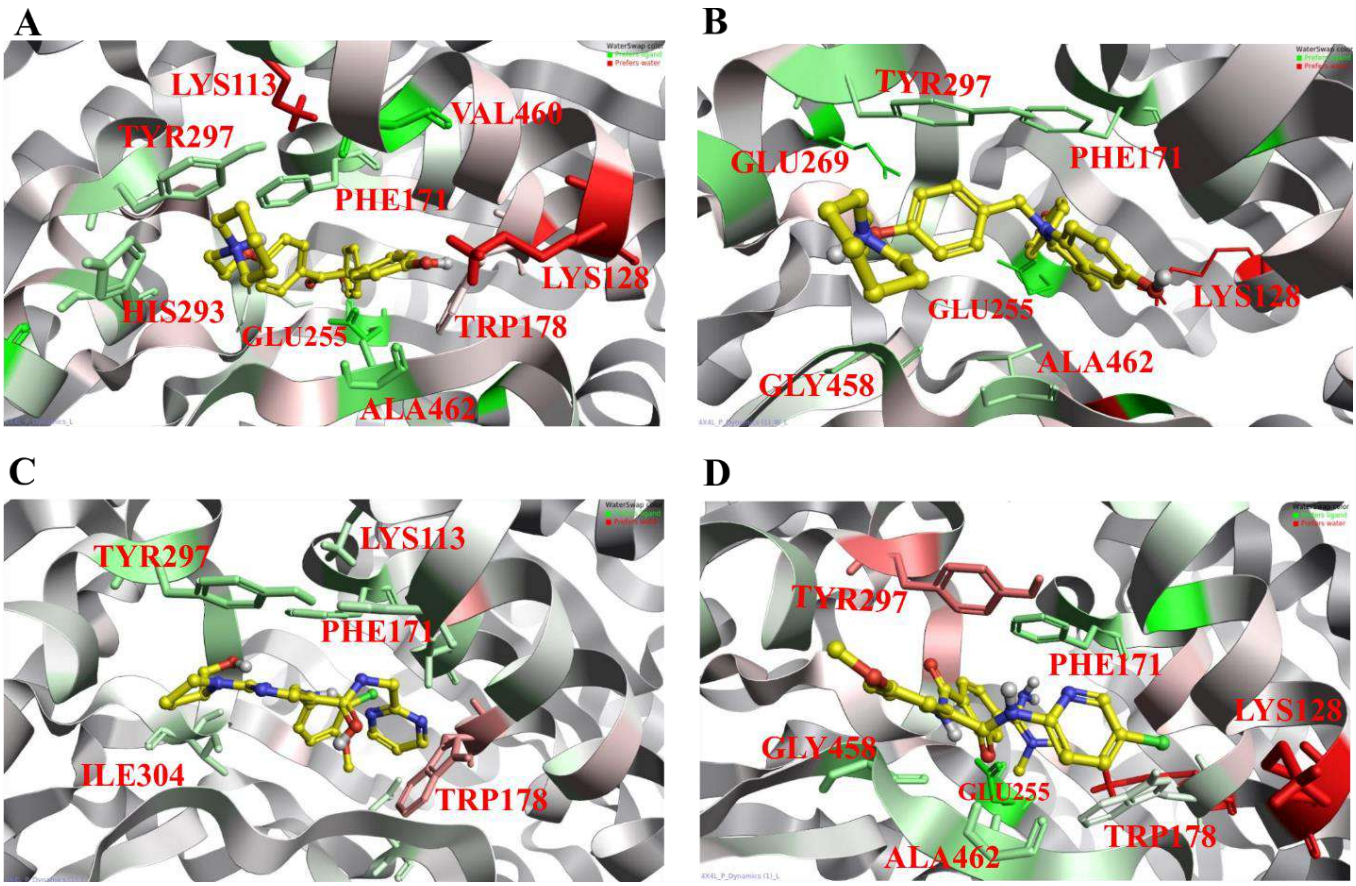

Figure 10: ALDH1A1 active site residues favorable to the ligand interactions are shown in green, the darker the green is, the more favorable, and residues unfavorable to ligand binding are shown in red. **A**) raloxifene, **B**) bazedoxifene, **C**) betrixaban, **D**) avanafil.

Table 4: Binding energies calculated using WaterSwap analysis

Drug Name	Bennett	FEP*	TI#	TI Quadratic	The consensus of Arthematic mean (kcal/mol)
Raloxifene	-40.30	-41.13	-39.10	-37.57	-42.00
Bazedoxifene	-39.73	-37.26	-36.30	-38.84	-38.03
Avanafil	-11.99	-13.75	-15.24	-14.31	-13.82
Betrixaban	-10.40	-9.62	-12.36	-13.57	-11.48

*Free energy perturbation

#Thermodynamics integration

4.4. *In-vitro* enzymatic assay

The inhibitory effects of the screened drugs, including raloxifene, bazedoxifene, avanafil, and betrixaban against recombinant human ALDH1A1, ALDH2, and ALDH3A1 were measured according to the protocol reported in previous reports [22]. Of these, both raloxifene and bazedoxifene were identified as the most promising drugs as ALDH1A1 selective inhibitors over avanafil and betrixaban. The detailed % inhibition of all the drugs with different ALDH isoforms has been displayed in **Fig. 10A, B,** and **C**. Then the IC_{50} values were calculated using the ATT bioquest IC_{50} calculator (https://www.aatbio.com/tools/ic50-calculator). From the evaluated results it was concluded that all the tested compounds exhibited good inhibitory activity against ALDH1A1 with IC_{50} values in the range of µM concentrations (**Table 5**). As shown in **Table 5**, raloxifene and bazedoxifene were found to inhibit ALDH1A1 at 2.35 µM and 4.41 µM, respectively, while the same drugs did not possess any inhibitory activity toward the rest of the isoforms, i.e., ALDH2 and ALDH3A1 at 100 µM. Meanwhile, avanafil and betrixaban did not possess any activity against ALDH1A1 at the given concentration (10 µM), and the drugs showed inhibitory potentials against ALDH2 and ALDH3A1 at higher concentrations. In addition, the reference NCT-501 shows 0.9 µM inhibitory potential against ALDH1A1 and did not possess any activity towards ALDH2 and ALDH3A1.

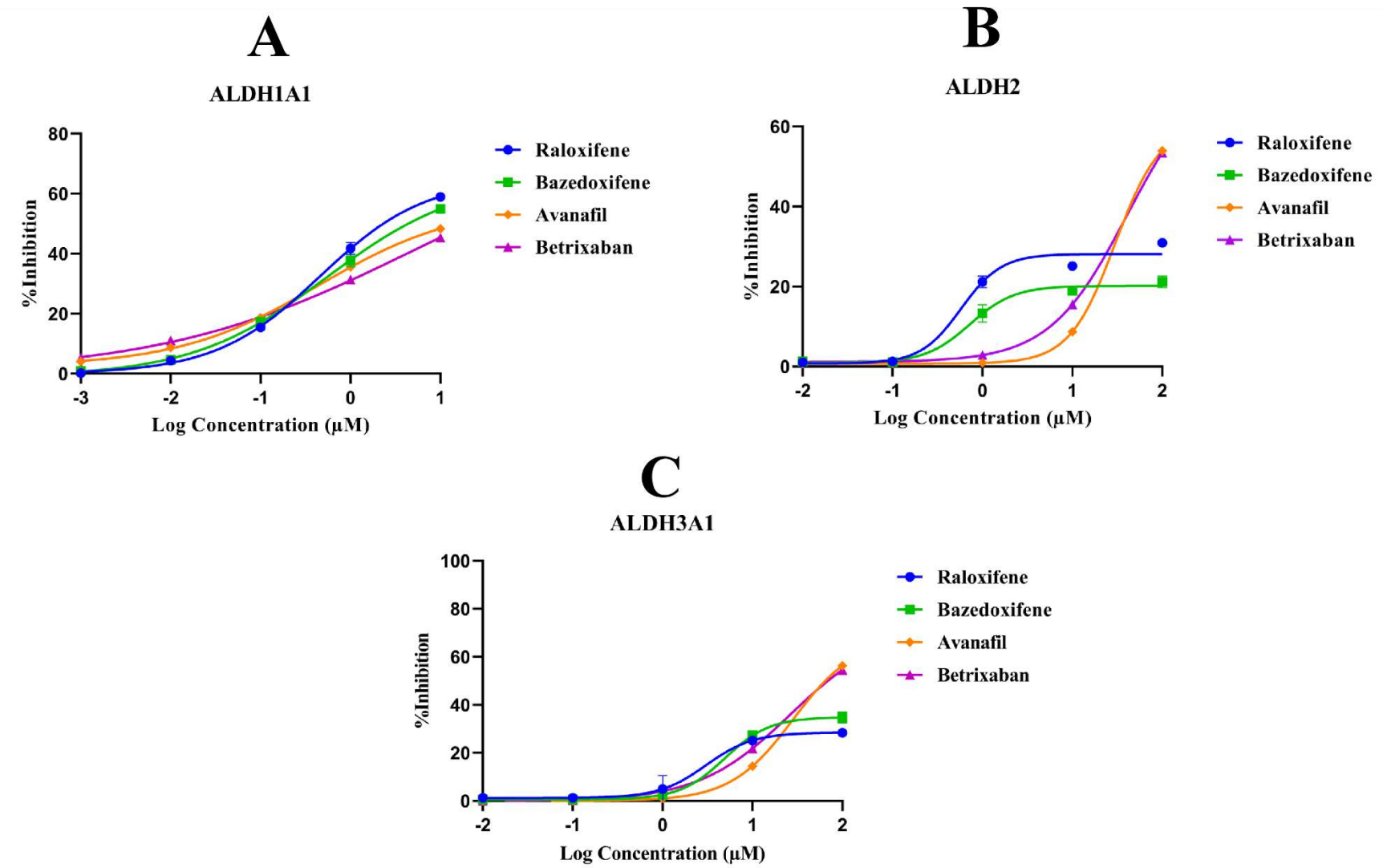

Figure 10: Concentration response curve to identify % inhibition **A**) ALDH1A1, **B**) ALDH2, and **C**) ALDH3A1; **D**) *In-vitro* activity results indicating IC_{50} of FDA drug for ALDH1A1, ALDH2, and ALDH3A1

Table 5: ALDH isoforms inhibition by raloxifene, bazedoxifene, avanafil, and betrixaban.

S. No.	Compound Name	ALDH IC_{50} (µM) ±SD[$]		
		ALDH1A1	**ALDH2**	**ALDH3A1**
1.	Raloxifene	2.35±0.45	>100(NI[*])	>100
2.	Bazedoxifene	4.41±0.50	>100	>100
3.	Avanafil	>10	73.38±3.86	64.72±5.77
4.	Betrixaban	>10	79.71±3.79	69.28±4.81
5.	NCT-501 (Reference)	0.9±0.42	>100	>100

[*]No inhibition

[$]Standard deviation

3.5. Mafosfamide sensitivity assays

As discussed in the methodology section, two cell lines, A549 and MIA PaCa-2 were used in the present study to identify maf sensitivity with the combination of raloxifene and bazedoxifene. These FDA-approved drugs were selected because they manifested greater inhibition and selectivity toward ALDH1A1 in the enzymatic assay studies. The obtained MTT results were expressed as % growth inhibition (Mean ± S. D.) v/s different concentrations of the FDA compounds + fixed concentration of maf ((i. e. half of the IC_{50} (138.04 for A549) and (128.08 for MIA PaCa-2) obtained individually)). As shown in **Fig. 11A and B** the cytotoxicity effect of maf on A549 and MIA-PaCa-2 was significantly improved with the combination of treatment with maf + raloxifene compared to maf alone. Similarly, the cytotoxicity of maf on A549 was also improved by the combination of maf + bazedoxifene than maf alone, while the same combination indicates no cytotoxicity effect on MIA PaCa-2 at the given concentrations. The graphs also clearly indicate that an increase in the concentration of raloxifene and bazedoxifene led to a reduction in cell growth viability. In addition, treatment of A549 and MIA PaCa-2 cells with maf in the presence of reference compounds i.e. NCT-501 showed a marked increase in maf sensitivity compared to

maf alone. The antiproliferative potentials of FDA-approved drugs, such as raloxifene and bazedoxifene alone and in combination with maf were compared to reference compound NCT-501 **(Table 6)**. The results indicated that the repurposed drugs alone indicated antiproliferative activity in both cell lines. The maf alone possesses poor antiproliferative activity towards both cell lines. However, the combination of raloxifene and bazedoxifene with maf showed the highest maf chemosensitivity than maf alone on both cell lines. These results indicate that the use of bazedoxifene and raloxifene with maf at low concentrations could eliminate the resistance. Also, the combination enhances the maf sensitivity in ALDH1A1-overexpressing tumor types.

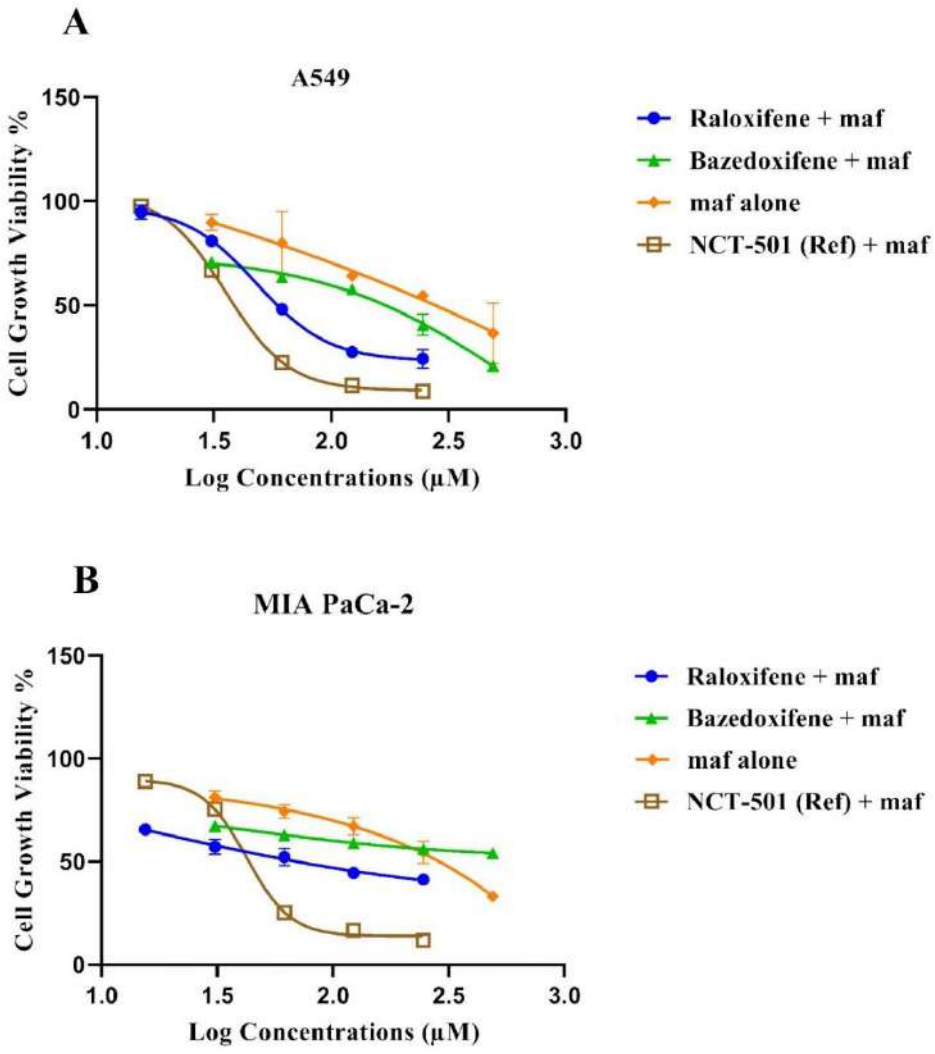

Figure. 11: Mafosfamide sensitivity assay in **A**) A549 and **B**) MIA PaCa-2 cells

Table 6: *In-vitro* antiproliferative activity of Identified drugs alone and in combination with maf using A549 and MIA PaCa-2 cell lines

S. No.	Drugs (Alone/Combination)	A549 cell line (IC_{50} (µM) ± SD)	MIA PaCa-2 cell line (IC_{50} (µM) ± SD)
1.	Raloxifene alone	91.18±0.21	188.32±0.12
2.	Bazedoxifene alone	371.32±0.11	385.23±0.32
3.	NCT-501 alone	68.92±0.56	179.55±0.65
4.	Maf alone	276.09±1.25	256.17±2.10
5.	Raloxifene + Maf	71.71±0.01	79.66±0.05
6.	Bazedoxifene + Maf	130.60±0.12	>500±0.01
7.	NCT-501 + Maf	38.55±0.32	60.25±0.24

5. Discussion

Drug resistance is one of the most common causes of cancer therapeutic failure. Changes in drug uptake or efflux rates, target mutations, gene amplification, enhanced DNA repair, and overexpression of DMEs are a few resistance mechanisms. Among them, DME-mediated chemoresistance is one of the most overlooked causes that has become a target of interest for researchers. CP, one of the important and most prescribed chemotherapeutics, is reported to undergo inactivation to an inactive metabolite via a DME known as ALDH1A1. Moreover, its clinical utility is often limited by bone marrow toxicity especially when it is administered in higher doses in resistance conditions [39]. Thus, the development of novel ALDH1A1 inhibitors can overcome both CP resistance and toxicity problems.

In the present study, a drug repurposing approach was carried out to screen some approved drugs as selective ALDH1A1 inhibitors. Herein this approach has been implemented to identify approved drugs as selective ALDH1A1 inhibitors with well-established safety, pharmacokinetics, and toxicity profiles, which is a great issue for most of the reported inhibitors of this target. Considering already published machine learning models against the targets ALDH1A1, ALDH2, and ALDH3A1 by our research group, a total of 115 molecules were scrutinized as selective ALDH1A1 inhibitors. Among the obtained hits, four drugs, raloxifene, bazedoxifene, avanafil, and betrixaban, were considered for MD simulation based on their compromised docking scores against ALDH isoforms, i.e., ALDH2 and ALDH3A1. Raloxifene and bazedoxifene are selective estrogen receptor modulators [40]. Raloxifene is primarily used to prevent osteoporosis in postmenopausal women, and bazedoxifene is used to treat hot flushes in women during menopause [41, 42]. The two drug molecules share high structural similarities with previously reported selective ALDH1A1 inhibitors by Li et. al., and Yang et al., [23, 37]. In addition, these drugs show good binding interactions with important amino acids responsible for ALDH1A1 inhibition along with high binding energy scores. These results encouraged to subject of these drugs for further *in-vitro* enzymatic assay studies. The IC50 values for raloxifene and bazedoxifene were found to be 2.35 µM and 4.41 µM by inhibition assays, respectively. However, due to surface topography dissimilarity among the ALDH isoforms, neither raloxifene nor bazedoxifene exhibited any inhibitory activity against ALDH2 and ALDH3A1. As per Morgan and Hurley, molecules showing steric clashes with residues, including Asp458 of ALDH2 and Ile458 of ALDH3A1, prohibit the

compounds from inhibiting these enzymes [43]. A similar kind of observation was identified in the present study. Both raloxifene and bazedoxifene demonstrated strong clashes with the bulky amino acids in ALDH2 and ALDH3A1. Moreover, bazedoxifene show some additional steric clashes with other bulky amino acids present on the surface of ALDH3A1, the details were provided in the supplementary file. The final obtained molecules had specific features and structural shapes that fit into ALDH1A1 and possessed the ability to bind to its wider active site. The narrow entry pathways of both ALDH2 and ALDH3A1 eliminate the possibility of binding of raloxifene and bazedoxifene. These *in-silico* results were in corollary to *in-vitro* enzymatic inhibition studies where raloxifene and bazedoxifene showed selective inhibition against ALDH1A1 and weak inhibition against ALDH2 and ALDH3A1. Some of the already reported literature evidence indicate that raloxifene and bazedoxifene are used in cancer treatment [44-46]. In particular, raloxifene is approved for invasive breast cancer in postmenopausal women. Its combination with other anticancer drugs has also been reported to have optimal therapeutic effects. A combination of raloxifene and letrozole has been reported to possess an additive cytotoxic effect in the MCF-7-cell line [47]. Similarly, the combination of raloxifene and conjugated estrogen has been reported to reduce the severity of menopausal symptoms [48]. The effect of the combination of raloxifene and CP has not yet been reported, the drug-drug interaction information deposited in the drug bank supports the fact that the metabolism of CP decreased when combined (https://go.drugbank.com/drugs/DB00481) with raloxifene. In addition, a study by Zhong et. al. confirmed that raloxifene shows the inhibition of recombinant ALDH1A1 [49]. Likewise, bazedoxifene can also be used in a variety of cancers, including breast cancer, pancreatic cancer, and gastric cancer [50-52]. Moreover, in the present investigation, both drugs found here that raloxifene and bazedoxifene could inhibit ALDH1A1, so the combination of these drugs with CP may be beneficial for the CP resistance problem.

Avanafil and betrixaban are other FDA drugs obtained from VS as ALDH1A1 inhibitors. Both drugs were found to inhibit ALDH1A1 with an IC_{50} value of >10 µM. Moreover, these drugs also showed inhibitory activity against ALDH2 and ALDH3A1 with higher IC_{50} values (>100 µM) than ALDH1A1. This is might be due to their pi-pi interactions with the ALDH2 and ALDH3A1 surface amino acids. However, the molecules still have greater IC_{50} (>10) values toward ALDH1A1. Therefore, the best-identified raloxifene and bazedoxifene were further considered for cell line studies.

The influence of ALDH1A1 inhibitors on the anticancer activity of maf was examined in A549 and MIA PaCa-2 cell lines. A significant increase in sensitivity toward maf was observed when given in the combination with raloxifene and bazedoxifene. However, the maf sensitivity in the above case is not higher than what was observed with the combination of maf and standard ALDH1A1 inhibitor (NCT-501). But, as described in the introduction NCT-501 has a lower half-life i.e., <1hr. Therefore, the obtained FDA molecules with known pharmacokinetics are more beneficial than the standard ones. Moreover, the FDA molecules show optimal maf sensitivity in both cell lines. Thus, both raloxifene and bazedoxifene could be the solution to the CP resistance.

6. Conclusion

To ameliorate the problem associated with CP resistance owing to ALDH1A1 in cancer cell lines, herein drug repurposing approach is implemented using various ligand and structure-based drug designing methods including machine learning, molecular docking, and dynamics study. Implementing the aforementioned approaches, two of the FDA-approved drugs raloxifene and bazedoxifene are predicted to be potential selective ALDH1A1 inhibitors. This type of observation was also validated by an *in-vitro* enzymatic assay in which both the drugs manifested IC_{50} values of 2.35±0.45μM and 4.41±0.50 μM, respectively against ALDH1A1 with no inhibition against ALDH2 and ALDH3A1 at 100 μM. The cell line assay against A549 and Mia-PaCa-2 cells also demonstrated the ability of both these drugs in combination with maf (analog of CP) to reverse the CP resistance. The selectivity of these two drugs towards ALDH1A1 over ALDH2 and ALDH3A1 could be explained based on molecular docking. This computational approach revealed that both Raloxifene and bazedoxifene showed selectivity toward ALDH1A1 and no inhibition at 100 μM toward ALDH2 and ALDH3A1 due to steric clashes with residues, such as Asp458 of ALDH2 and Ile458 of ALDH3A1. These new scaffolds may be a good starting point for designing more ALDH1A1 inhibitors as adjuvant therapy for CP resistance correlated with ALDH1A1 overexpression. In addition, the drugs can take for further evaluation in other cell lines that could overexpress ALDH1A1 and also *in-vivo* evaluation for stronger evidence about the combinations.

References

[1] M. Ahlmann, G. Hempel, The effect of cyclophosphamide on the immune system: implications for clinical cancer therapy, Cancer Chemother. Pharmacol. 78 (2016) 661-671.

[2] A.P. Tran, M. Ali Al-Radhawi, I. Kareva, J. Wu, D.J. Waxman, E.D. Sontag, Delicate balances in cancer chemotherapy: Modeling immune recruitment and emergence of systemic drug resistance, Front. Immunol. (2020) 1376.
[3] X. Wang, H. Zhang, X. Chen, Drug resistance and combating drug resistance in cancer, Cancer drug resist. 2 (2019) 141.
[4] M. Kartal-Yandim, A. Adan-Gokbulut, Y. Baran, Molecular mechanisms of drug resistance and its reversal in cancer, Crit. Rev. Biotechnol. 36(4) (2016) 716-726.
[5] B. Raju, H. Verma, G. Narendra, B. Sapra, O. Silakari, Multiple machine learning, molecular docking, and ADMET screening approach for identification of selective inhibitors of CYP1B1, J. Biomol. Struct. Dyn. (2021) 1-16.
[6] H. Verma, M. Singh Bahia, S. Choudhary, P. Kumar Singh, O. Silakari, Drug metabolizing enzymes-associated chemo resistance and strategies to overcome it, Drug Metab. Rev. 51(2) (2019) 196-223.
[7] B. Jackson, C. Brocker, D.C. Thompson, W. Black, K. Vasiliou, D.W. Nebert, V. Vasiliou, Update on the aldehyde dehydrogenase gene (ALDH) superfamily, Hum. Genomics 5(4) (2011) 1-21.
[8] V. Vasiliou, D.W. Nebert, Analysis and update of the human aldehyde dehydrogenase (ALDH) gene family, Hum. Genomics 2(2) (2005) 1-6.
[9] S.A. Marchitti, R.A. Deitrich, V. Vasiliou, Neurotoxicity and metabolism of the catecholamine-derived 3, 4-dihydroxyphenylacetaldehyde and 3, 4-dihydroxyphenylglycolaldehyde: the role of aldehyde dehydrogenase, Pharmacol. Rev. 59(2) (2007) 125-150.
[10] C. Smith, M. Gasparetto, C. Jordan, D.A. Pollyea, V. Vasiliou, The effects of alcohol and aldehyde dehydrogenases on disorders of hematopoiesis, Biological Basis of Alcohol-Induced Cancer (2015) 349-359.
[11] W. Wang, C. Wang, H. Xu, Y. Gao, Aldehyde dehydrogenase, liver disease and cancer, Int. J. Biol. Sci. 16(6) (2020) 921.
[12] M. Magni, S. Shammah, R. Schiró, W. Mellado, R. Dalla-Favera, A.M. Gianni, Induction of cyclophosphamide-resistance by aldehyde-dehydrogenase gene transfer, (1996).

[13] J. Zhang, Q. Tian, S. Yung Chan, S. Chuen Li, S. Zhou, W. Duan, Y.-Z. Zhu, Metabolism and transport of oxazaphosphorines and the clinical implications, Drug Metab. Rev. 37(4) (2005) 611-703.
[14] B. Raju, S. Choudhary, G. Narendra, H. Verma, O. Silakari, Molecular modeling approaches to address drug-metabolizing enzymes (DMEs) mediated chemoresistance: a review, Drug Metab. Rev. 53(1) (2021) 45-75.
[15] X. He, Y. Deng, W. Yue, Investigating critical genes and gene interaction networks that mediate cyclophosphamide sensitivity in chronic myelogenous leukemia, Mol. Med. Rep. 16(1) (2017) 523-532.
[16] H. Verma, O. Silakari, Investigating the Role of Missense SNPs on ALDH 1A1 mediated pharmacokinetic resistance to cyclophosphamide, Comput. Biol. Med. 125 (2020) 103979.
[17] G. Narendra, B. Raju, H. Verma, O. Silakari, Identification of potential genes associated with ALDH1A1 overexpression and cyclophosphamide resistance in chronic myelogenous leukemia using network analysis, Med. Oncol. 38(10) (2021) 1-10.
[18] G.G. Muramoto, J.L. Russell, R. Safi, A.B. Salter, H.A. Himburg, P. Daher, S.K. Meadows, P. Doan, R.W. Storms, N.J. Chao, Inhibition of aldehyde dehydrogenase expands hematopoietic stem cells with radioprotective capacity, Stem cells 28(3) (2010) 523-534.
[19] S.-M. Yang, A. Yasgar, B. Miller, M. Lal-Nag, K. Brimacombe, X. Hu, H. Sun, A. Wang, X. Xu, K. Nguyen, Discovery of NCT-501, a potent and selective theophylline-based inhibitor of aldehyde dehydrogenase 1A1 (ALDH1A1), J. Med. Chem. 58(15) (2015) 5967-5978.
[20] A.C. Kimble-Hill, B. Parajuli, C.-H. Chen, D. Mochly-Rosen, T.D. Hurley, Development of selective inhibitors for aldehyde dehydrogenases based on substituted indole-2, 3-diones, J. med. chem. 57(3) (2014) 714-722.
[21] C.D. Buchman, K.K. Mahalingan, T.D. Hurley, Discovery of a series of aromatic lactones as ALDH1/2-directed inhibitors, Chem. Biol. Interact. 234 (2015) 38-44.
[22] C.A. Morgan, T.D. Hurley, Characterization of two distinct structural classes of selective aldehyde dehydrogenase 1A1 inhibitors, J. med. chem. 58(4) (2015) 1964-1975.
[23] S.-M. Yang, N.J. Martinez, A. Yasgar, C. Danchik, C. Johansson, Y. Wang, B. Baljinnyam, A.Q. Wang, X. Xu, P. Shah, Discovery of orally bioavailable, quinoline-based aldehyde dehydrogenase 1A1 (ALDH1A1) inhibitors with potent cellular activity, J. med. chem. 61(11) (2018) 4883-4903.

[24] C. Anorma, J. Hedhli, T.E. Bearrood, N.W. Pino, S.H. Gardner, H. Inaba, P. Zhang, Y. Li, D. Feng, S.E. Dibrell, Surveillance of cancer stem cell plasticity using an isoform-selective fluorescent probe for aldehyde dehydrogenase 1A1, ACS Cent. Sci. 4(8) (2018) 1045-1055.
[25] L. Sleire, H.E. Førde, I.A. Netland, L. Leiss, B.S. Skeie, P.Ø. Enger, Drug repurposing in cancer, Pharmacol. Res. 124 (2017) 74-91.
[26] N. Kumar, A. Gahlawat, R.N. Kumar, Y.P. Singh, G. Modi, P. Garg, Drug repurposing for Alzheimer's disease: in silico and in vitro investigation of FDA-approved drugs as acetylcholinesterase inhibitors, J. Biomol. Struct. Dyn. (2020) 1-15.
[27] C.G. Begley, M. Ashton, J. Baell, M. Bettess, M.P. Brown, B. Carter, W.N. Charman, C. Davis, S. Fisher, I. Frazer, Drug repurposing: Misconceptions, challenges, and opportunities for academic researchers, Sci. Transl. Med. 13(612) (2021) eabd5524.
[28] G. Narendra, B. Raju, H. Verma, B. Sapra, O. Silakari, Multiple machine learning models combined with virtual screening and molecular docking to identify selective human ALDH1A1 inhibitors, J. Mol. Graph. Model. 107 (2021) 107950.
[29] J.J. Irwin, B.K. Shoichet, ZINC− a free database of commercially available compounds for virtual screening, J. Chem. Inf. Model. 45(1) (2005) 177-182.
[30] C.W. Yap, PaDEL-descriptor: An open source software to calculate molecular descriptors and fingerprints, J. Comput. Chem. 32(7) (2011) 1466-1474.
[31] H.M. Berman, J. Westbrook, Z. Feng, G. Gilliland, T.N. Bhat, H. Weissig, I.N. Shindyalov, P.E. Bourne, The protein data bank, Nucleic Acids Res. 28(1) (2000) 235-242.
[32] G. Kiran, L. Karthik, M.S. Devi, P. Sathiyarajeswaran, K. Kanakavalli, K. Kumar, D.R. Kumar, In silico computational screening of Kabasura Kudineer-official Siddha formulation and JACOM against SARS-CoV-2 spike protein, J. Ayurveda Integr. Med. (2020) 100324.
[33] C.J. Woods, M. Malaisree, S. Hannongbua, A.J. Mulholland, A water-swap reaction coordinate for the calculation of absolute protein–ligand binding free energies, J. Chem. Phys. 134(5) (2011) 02B611.
[34] C.J. Woods, M. Malaisree, J. Michel, B. Long, S. McIntosh-Smith, A.J. Mulholland, Rapid decomposition and visualisation of protein–ligand binding free energies by residue and by water, Faraday Discuss. 169 (2014) 477-499.
[35] A. Yasgar, S.A. Titus, Y. Wang, C. Danchik, S.-M. Yang, V. Vasiliou, A. Jadhav, D.J. Maloney, A. Simeonov, N.J. Martinez, A high-content assay enables the automated screening and

identification of small molecules with specific ALDH1A1-inhibitory activity, PLoS One 12(1) (2017) e0170937.
[36] B. Parajuli, M.L. Fishel, T.D. Hurley, Selective ALDH3A1 inhibition by benzimidazole analogues increase mafosfamide sensitivity in cancer cells, J. med. chem. 57(2) (2014) 449-461.
[37] B. Li, K. Yang, D. Liang, C. Jiang, Z. Ma, Discovery and development of selective aldehyde dehydrogenase 1A1 (ALDH1A1) inhibitors, Eur. J. Med. Chem. 209 (2021) 112940.
[38] H. Verma, G. Narendra, B. Raju, M. Kumar, S.K. Jain, G.K. Tung, P.K. Singh, O. Silakari, 3D-QSAR and scaffold hopping based designing of benzo [d] ox-azol-2 (3H)-one and 2-oxazolo [4, 5-b] pyridin-2 (3H)-one derivatives as selective aldehyde dehydrogenase 1A1 inhibitors: Synthesis and biological evaluation, Arch. Pharm. (2022) e2200108.
[39] R. Brown, R. Herzig, S. Wolff, D. Frei-Lahr, L. Pineiro, B. Bolwell, J. Lowder, E. Harden, K. Hande, G. Herzig, High-dose etoposide and cyclophosphamide without bone marrow transplantation for resistant hematologic malignancy, (1990).
[40] J.H. Pickar, B.S. Komm, Selective estrogen receptor modulators and the combination therapy conjugated estrogens/bazedoxifene: a review of effects on the breast, Post reprod. health 21(3) (2015) 112-121.
[41] B. Ettinger, D.M. Black, B.H. Mitlak, R.K. Knickerbocker, T. Nickelsen, H.K. Genant, C. Christiansen, P.D. Delmas, J.R. Zanchetta, J. Stakkestad, Reduction of vertebral fracture risk in postmenopausal women with osteoporosis treated with raloxifene: results from a 3-year randomized clinical trial, Jama 282(7) (1999) 637-645.
[42] W. Utian, H. Yu, J. Bobula, S. Mirkin, S. Olivier, J.H. Pickar, Bazedoxifene/conjugated estrogens and quality of life in postmenopausal women, Maturitas 63(4) (2009) 329-335.
[43] C.A. Morgan, T.D. Hurley, Development of a high-throughput in vitro assay to identify selective inhibitors for human ALDH1A1, Chem. Biol. Interact. 234 (2015) 29-37.
[44] E. Zafar, M.F. Maqbool, A. Iqbal, A. Maryam, H.A. Shakir, M. Irfan, M. Khan, Y. Li, T. Ma, A comprehensive review on anticancer mechanism of bazedoxifene, Biotechnol. Appl. Biochem. 69(2) (2022) 767-782.
[45] S. Goldstein, Selective estrogen receptor modulators and bone health, Climacteric 25(1) (2022) 56-59.
[46] T.-H. Heo, J. Wahler, N. Suh, Potential therapeutic implications of IL-6/IL-6R/gp130-targeting agents in breast cancer, Oncotarget 7(13) (2016) 15460.

[47] D. Vohora, A. Kalam, A. Leekha, S. Talegaonkar, A.K. Verma, Combined raloxifene and letrozole for breast cancer patients, Arch. Med. Res. 48(6) (2017) 561-565.
[48] A.L.B. Carneiro, A.P.C. Spadella, F.A.d. Souza, K.B.F. Alves, J.T.d. Araujo-Neto, M.A. Haidar, R.d.C.d.M. Dardes, Effects of Raloxifene Combined with Low-dose Conjugated Estrogen on the Endometrium in Menopausal Women at High Risk for Breast Cancer, Clinics 76 (2021).
[49] G. Zhong, C.J. Seaman, E.M. Paragas, H. Xi, K.-L. Herpoldt, N.P. King, J.P. Jones, N. Isoherranen, Aldehyde oxidase contributes to all-trans-retinoic acid biosynthesis in human liver, Drug Metab. Dispos. 49(3) (2021) 202-211.
[50] C. Burkhardt, L. Bühler, M. Tihy, P. Morel, M. Forni, Bazedoxifene as a novel strategy for treatment of pancreatic and gastric adenocarcinoma, Oncotarget 10(34) (2019) 3198.
[51] R. Zhang, T. Wang, J. Lin, Synergistic effect of bazedoxifene and PARP inhibitor in the treatment of ovarian cancer regardless of BRCA mutation, Anticancer Res. 41(5) (2021) 2277-2286.
[52] J. Tian, X. Chen, S. Fu, R. Zhang, L. Pan, Y. Cao, X. Wu, H. Xiao, H.-J. Lin, H.-W. Lo, Bazedoxifene is a novel IL-6/GP130 inhibitor for treating triple-negative breast cancer, Breast Cancer Res. Treat. 175(3) (2019) 553-566.